

Self-Organization in Interface Dynamics and Urban Development

EHUD MERON

*The Jacob Blaustein Institute for Desert Research and The Physics Department,
Ben-Gurion University, Sede Boker Campus 84990, Israel*

(Received 16 November 1998)

The view of the urban environment as an extended nonlinear system introduces new concepts, motivates new questions, and suggests new methodologies in the study of urban dynamics. A review of recent results on interface dynamics in nonequilibrium physical systems is presented, and possible implications on the urban environment are discussed. It is suggested that the growth modes of specific urban zones (e.g. residential, commercial, or industrial) and the factors affecting them can be studied using mathematical models that capture two generic interface instabilities.

Keywords: Interfaces, Nonlinear dynamics, Urban environments, Instabilities

1 INTRODUCTION

The urban environment resembles in many respects a dissipative physical system maintained out of equilibrium by influx and outflux of energy and matter [1,2]. A living system is perhaps the first example to come to mind but more instructive for our purposes is the example of a chemical reaction continuously refreshed with new chemicals. Despite the enormous number of matter constituents, the atoms and molecules, the overall behavior of such a system can be surprisingly coherent; the system may self-organize into spatiotemporal patterns of chemical concentrations. Figure 1 shows the development of a labyrinthine pattern in a chemical reaction studied by Swinney and coworkers [3,4].

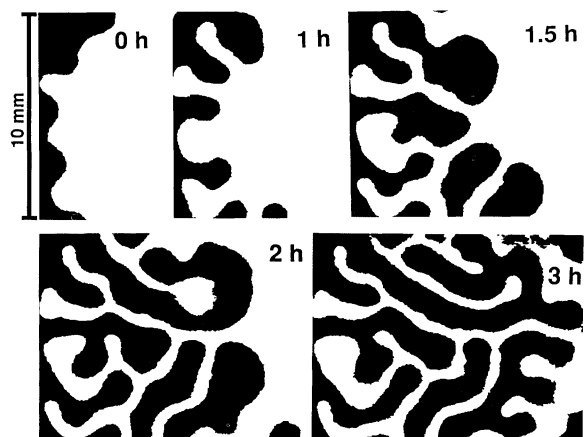


FIGURE 1 The development of a labyrinthine pattern in a chemical reaction due to an interface instability (from Lee *et al.* [3], reproduced with permission).

The dark region, pertaining to high acidity, invades into the light region (low acidity) by growing fingers, leaving a mixed dark–light pattern. The driving force that maintains this pattern is the continuous supply of chemicals which replace those consumed. The latter turn into products that leave the reaction scene.

Similarly, the urban environment can be viewed as a far from equilibrium system driven by a continuous inflow of information, raw materials or residents, and sustaining patterns of commercial zones, industrial zones, socioeconomic residential areas, and so on. Adopting this view Portugali *et al.* have recently used discrete mathematical models to study spatiotemporal patterns of sociocultural segregation. Their City model [5] consists of a two-dimensional square lattice of cells, each of which is conceived as a house or a place in the urban environment. Any given place is assigned a state, it may be vacant or occupied by individuals of different sociocultural backgrounds, denoted “blue” and “green”. An instantaneous state of the city is given by the state matrix of all cells. The temporal evolution of the city is dictated by a set of rules defining the state of any given place at the next time step as a function of the current states of the cell itself and its nearest neighbors. Computer simulations of the model yield patterns consisting of green and blue domains. Changing the rules affects the patterns and allows assessing the effects of various factors on the sociocultural structure of the City.

Discrete models of this nature fall in the class of Cellular Automaton (CA) models [6], which have been used in a variety of physical contexts including hydrodynamics and chemical reactions [7,8]. CA models have successfully reproduced various nonlinear behaviors of these systems, and from a computational point of view, provide economical substitutes for the pertinent nonlinear partial differential equations, the Navier Stokes equations for fluids, and reaction–diffusion equations for chemical systems. In the context of urban development CA models are natural choices [5], for partial differential equations are difficult to motivate

(see however [9]) and the consideration of urban factors is most readily done at the discrete cellular level.

The temporal evolution of domain patterns, such as the chemical patterns shown in Fig. 1 or the segregation patterns exhibited by the City model, is strongly affected by the dynamics of the interface between the different domains, low and high acidity or blue and green residential areas. The main purpose of this paper is to expose urban researchers to recent developments in nonequilibrium interface dynamics, and to address possible implications on the urban environment. We will focus on two generic interface instabilities, an instability to transverse perturbations and a parity breaking bifurcation, and discuss the different growth modes associated with them.

We begin in Section 2 with a review of basic concepts of nonlinear dynamics which we will need in the rest of the paper, and discuss their significance in the urban context. In Section 3 we analyze two interface instabilities using a two-variable reaction–diffusion model describe possible interface instabilities in nonequilibrium systems and study the effects they have on interface dynamics. Possible implications on the urban environment, and prospects for further developments in this new interdisciplinary area are discussed in Section 4.

2 DISSIPATIVE NONLINEAR DYNAMICS

Dynamical systems in nature can be divided into conservative and dissipative systems. The former conserve energy and obey dynamical equations of a very special (Hamiltonian) form. The latter are not restricted in this sense, and include physical systems that are open to energy exchanges with their environment, or systems for which the concept of energy is not well defined. Most dynamical systems in nature are also nonlinear. The nonlinear nature of a system may show up as a saturation of a growth process, as a driving force of a decaying process, or as a qualitative change in the system’s behavior as a control parameter is varied (see *bifurcation* below).

The urban environment justifiably falls in the class of dissipative nonlinear systems.

We illustrate basic properties of dissipative nonlinear systems [10] using the following nonlinear dynamical system for a single degree of freedom

$$\frac{du}{dt} = au - u^3 + b, \quad (1)$$

where t , the independent variable, represents time, $u(t)$ is a real dependent variable, and a, b are real constants. Consider first the case where $b=0$. The left hand side of (1) represents the rate of change of u . Let us look first at stationary solutions for which the rate of change is zero. Setting $du/dt=0$ leads (for $b=0$) to the equation $u(a-u^2)=0$. For $a < 0$ this equation has the single solution, $u=0$. For $a > 0$ two additional solutions exist, $u = \pm\sqrt{a}$. These stationary solutions demonstrate an important property of nonlinear systems. By varying a from negative to positive values a critical value is reached, $a=0$, where two new solutions, $u = \pm\sqrt{a}$ appear. We say that a *bifurcation* has occurred at $a=0$. This is an example of a parity breaking bifurcation; a parity symmetry, $u \rightarrow -u$, of (1) (for $b=0$) is broken by the solutions that exist for $a > 0$. The symmetry takes one solution into the other. It is instructive to plot the solutions of (1) as functions of the bifurcation parameter a . The resulting bifurcation diagram is shown in Fig. 2(a).

The bifurcation, as the figure suggests, is called a *pitchfork bifurcation*.

In order to understand the dynamical significance of the bifurcation at $a=0$ we need to study the *stability* of the various stationary solutions. Roughly speaking, we say that a given state is stable if small perturbations of this state decay to zero as time evolves. To study the stability of a stationary solution $u=u_0$ of (1) we write $u(t)=u_0+p(t)$, where $p(t)$ is an infinitesimal perturbation, and insert this form for u in (1). Neglecting nonlinear terms in p (p^2 and p^3) which are infinitesimally small in comparison with p , we find the linear equation

$$\frac{dp}{dt} = (a - 3u_0^2)p, \quad (2)$$

whose solution is $p(t) = p(0)e^{(a-3u_0^2)t}$, where $p(0)$ is the initial (at time $t=0$) value of the perturbation. For the stationary solution $u_0=0$, $p(t)=p(0)e^{at}$. Thus, for $a < 0$ the perturbation p decays to zero and the stationary solution $u_0=0$ is stable. For $a > 0$, p grows in time and $u_0=0$ is unstable. A similar consideration leads to the conclusion that the stationary states $u_0 = \pm\sqrt{a}$ which exist for $a > 0$ are stable. The stable (unstable) stationary solutions are indicated in the bifurcation diagram by solid (dashed) lines. Equation (1) for $a > 0$ is an example of a *bistable* system where two stable solutions coexist for given parameter values.

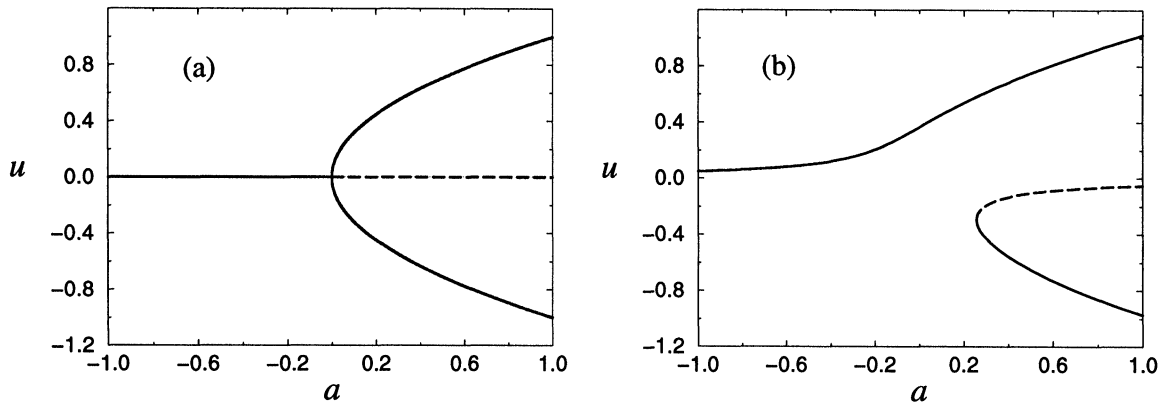


FIGURE 2 A pitchfork bifurcation diagram showing stationary solutions of Eq. (1) as functions of the control parameter a . (a) The symmetric case, $b=0$. (b) The asymmetric or imperfect case, $b=0.05$.

The stability analysis presented above refers to infinitesimally small perturbations, but the same conclusions hold for finite perturbations as well. Each of the stationary states has a *basin of attraction*, that is, a finite neighborhood within which all initial conditions converge to u_0 as $t \rightarrow \infty$. The basin of attraction of $u_0 = 0$ for $a < 0$ is the whole u axis, $-\infty < u < \infty$. For $a > 0$, u_0 is unstable and has no basin of attraction. The other two stationary states, $u_0 = -\sqrt{a}$ and $u_0 = \sqrt{a}$, have the basins of attraction $-\infty < u < 0$ and $0 < u < \infty$, respectively. Stable (unstable) solutions are often referred to as *attractors (repellors)* of the dynamics. The knowledge of all attractors and their basins of attraction allows, in principle, the determination of the attractor at which the system will eventually reside, given an initial condition. For example, for $a > 0$, any initial condition $u(0) < 0$ will lead to the attractor $u = -\sqrt{a}$ at $t \rightarrow \infty$.

When $b \neq 0$, the bifurcation diagram becomes asymmetric or *imperfect* as shown in Fig. 2(b). We may also plot the stationary solutions as functions of b for a given a . The outcome is shown in Fig. 3. Notice that for a positive a multivalued relation results. When a is small the upper and lower branches, pertaining to the two stable stationary states, terminate at small absolute values of b . This simple observation has far reaching consequences as we will see in the next section.

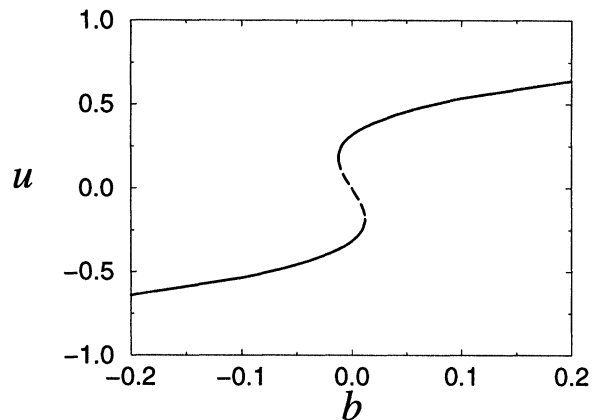


FIGURE 3 Stationary solutions of Eq. (1) with $a = 0.1$ as functions of the control parameter b .

Dynamical systems involving more than one degree of freedom may have additional types of stable solutions (besides stationary), and consequently different attractors of the dynamics. Systems containing two and more degrees of freedom may have stable periodic solutions in time, and systems having at least three degrees of freedom may exhibit *strange attractors* on which the dynamics are chaotic [10]. Spatially extended systems (described by partial differential equations rather than ordinary ones as (1)) exhibit attractors and repellors in the forms of spatial or spatio-temporal structures. We mention a few examples: (i) Stationary periodic patterns, i.e. solutions which are stationary in time and periodic in space. (ii) Periodic traveling waves, i.e. solutions which are periodic both in time and in space. (iii) Various localized structures such as fronts and vortices (see below and the next section).

The notion of attractors of the dynamics fits quite well our experience of urban dynamics. Consider for example two sociocultural groups residing in the same neighborhood. Ignoring for the moment the boundaries between the two groups, where cultural diffusion takes place, any individual in this neighborhood is likely to belong to one of the two cultures. Intermediate individuals, like newborn children or spouses from other cultures, will adopt in the course of time one culture or another depending on initial biases. In the terminology of nonlinear dynamics we may say that the two cultures form attractors of the dynamics and that initial conditions placed within the basin of attraction of a given culture will evolve to that culture as time goes to infinity. An individual may persist in an intermediate or mixed-culture state in the interface between the different sociocultural groups where diffusion of cultural influences takes place. Such an interface may also be an attractor of the dynamics in the sense that initial interface structures evolve toward a single stable interface with a characteristic width. This property is readily captured by adding a diffusion term to Eq. (1). We will discuss this modified equation in the next section.

We conclude this brief introduction emphasizing a property of nonlinear dissipative systems which we find significant in the context of urban studies. Bifurcation and instability phenomena and, consequently, the attractors associated with them, are universal. This explains why different physical processes, having very little in common like a chemical reaction and a fluid flow, may exhibit the same types of patterns, stripes, traveling waves, spiral waves and so on. The significance in the urban context is twofold. (i) The same attractors are expected to be found in urban dynamics, although complex urban dynamics may exhibit additional attractors not seen in relatively simple physical systems. (ii) In constructing models of urban development we need not take into account all possible factors; models with fewer factors may reproduce the same universal bifurcations, and therefore the same *qualitative* behaviors.

3 INTERFACE DYNAMICS IN CONTINUOUS SYSTEMS

An interface, in the context considered here, is a localized spatial structure forming a transition zone between two different stable uniform states of the system. The interface represents a stable balance between two competing processes, the tendency of the system to converge locally to one of the two states because of their stability, and diffusion. Without diffusion an infinitely sharp interface would form. The effect of diffusion is to smooth out the interface and give it a characteristic finite width. This can be readily seen by modifying Eq. (1) to include a diffusion term,

$$\frac{\partial u}{\partial t} = au - u^3 + b + D \frac{\partial^2 u}{\partial x^2}, \quad (3)$$

where D is a diffusion constant. The left hand side of (3) still represents the rate of change of u , but now at a given spatial location x . The last term on the right hand side represents the change of u at a given location due to diffusion into ($\partial^2 u / \partial x^2 > 0$) or out of ($\partial^2 u / \partial x^2 < 0$) that location.

Equation (3) has a stable interface or front solution, which for $b=0$ takes the simple stationary (non-propagating) form

$$u = \sqrt{a} \tanh \sqrt{\frac{a}{2D}} x. \quad (4)$$

As shown in Fig. 4 this solution connects the “down” state, $u = -\sqrt{a}$, at $x = -\infty$ to the “up” state, $u = \sqrt{a}$, at $x = \infty$. The width of the front (or interface) is proportional to $\sqrt{D/a}$. Thus, the interface becomes infinitely thin when diffusion vanishes ($D \rightarrow 0$).

Interfaces in systems *near* equilibrium are either stationary or propagating in a unique direction determined by the system’s parameters (we ignore at this stage the effect of interface curvature). In Eq. (3) the relevant parameter is b . The interface is stationary (propagating) for $b=0$ ($b \neq 0$). The direction of propagation is determined by the sign of b . The stationarity of the interface for $b=0$ is related to the parity symmetry $u \rightarrow -u$ of (3) which takes the up state $u = \sqrt{a}$ to the down state $u = -\sqrt{a}$, and vice versa. Systems maintained far from equilibrium may behave differently. Even when the up and down states are related by a symmetry, the interface connecting these states may propagate as discussed below.

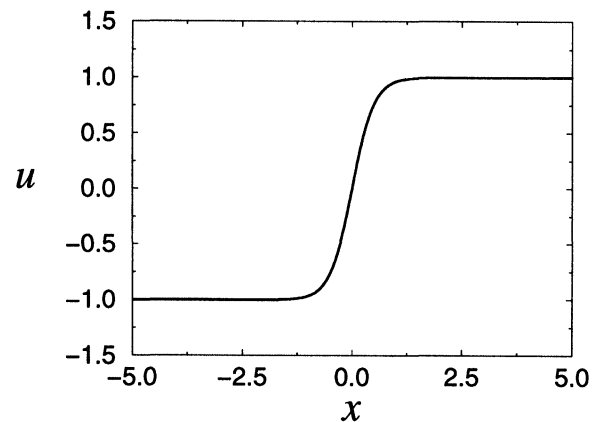


FIGURE 4 The stationary front solution (4) for $a=1$ and $D=0.125$.

3.1 A Pitchfork Front Bifurcation

Recent studies of various models representing nonequilibrium bistable systems [11–14] (see also the Appendix) have discovered a pitchfork *front* bifurcation as depicted in Fig. 5 (left). A stationary interface or front is stable only in a given range of parameter values, $\eta > \eta_c$. At $\eta = \eta_c$ the stationary front becomes unstable and a pair of propagating fronts appear, pertaining to an up state invading a down state (positive velocity) and a down state invading an up state (negative velocity). The counterpropagating fronts are stable and thus attractors of the dynamics. Breaking the parity symmetry between the up and down states yields the imperfect bifurcation diagram shown in Fig. 5 (right). Note that the direction of propagation for $\eta < \eta_c$ is not unique and determined by initial conditions rather than the sign of an asymmetry parameter like b in (1). In the Appendix we give a detailed derivation of a pitchfork front bifurcation for a particular reaction diffusion model. We just note that in order to have this front bifurcation a second dynamical variable (in addition to u) should be included in the model.

The coexistence of two interfaces moving in opposite directions beyond the bifurcation (i.e. for $\eta < \eta_c$) allows for the formation of spiral waves in two space dimensions. An interface between the

up and down states may be constructed so that one half of it corresponds to an up state invading a down state and the other half to a down state invading an up state. The twist action about the mid point induces rotational motion which evolves into a rotating spiral wave (or vortex) as shown in Fig. 6.

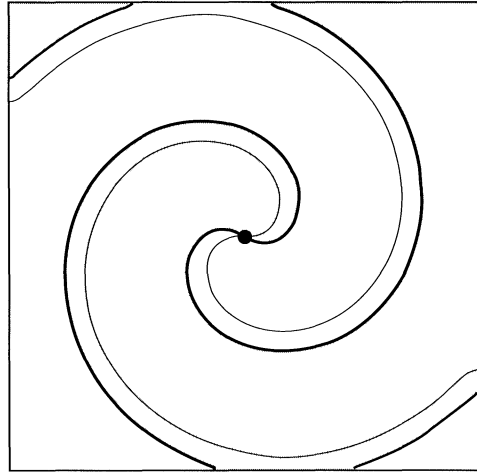


FIGURE 6 A rotating spiral wave obtained by numerical integration of (5) for $\eta < \eta_c$. The white and grey domains represent the up and down states, respectively. The thick line is the $u=0$ contour which represents the interface location. The thin line is the $v=0$ contour which contains information about the direction of propagation; it always lags behind the $u=0$ contour. The crossing point of the two lines is the center of rotation.

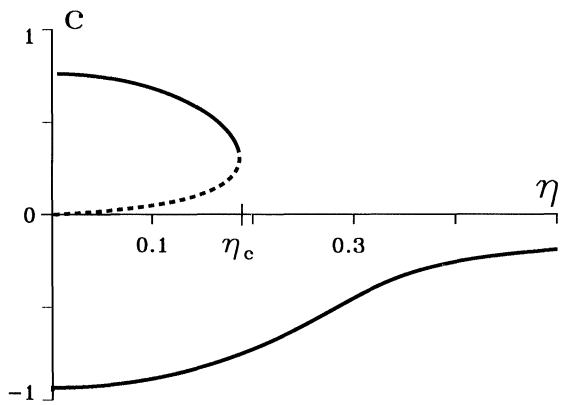
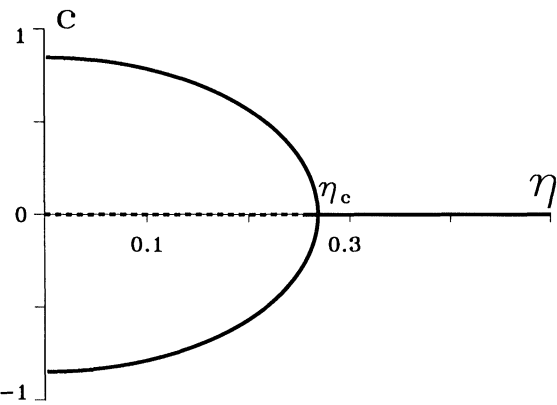


FIGURE 5 Pitchfork front bifurcations showing front solutions of Eq. (5) that propagate at constant velocities, c , as functions of the control parameter $\eta = (c\delta)^{1/2}$. The symmetric bifurcation for $a_0 = 0$ on the left, and the imperfect bifurcation for $a_0 = -0.1$ on the right.

Another interesting consequence of the front bifurcation is that small perturbations may induce transitions between the counterpropagating interfaces. Such perturbations play the role of the parameter b in Eq. (1), whose effect is displayed in Fig. 3. That is, the relation between the front velocity and the perturbation may become multi-valued (or hysteretic). Consider for example an interface propagating in two space dimensions. Very often the interface has a curvature which varies in time; we may think of an interface bounding a growing circular domain, whose curvature decreases in time. The curvature is an intrinsic perturbation (of a straight interface) and close to the front bifurcation affects the interface velocity as in Fig. 7 (see the Appendix). Imagine the growing domain is in the up state, and so the interface bounding it pertains to the upper branch of Fig. 8 (an up state invading a down state). As the domain grows the interface moves on the upper branch toward the end point (because curvature is decreasing). At a certain size this end point will be reached and an interface state corresponding to an up state invading a down state will no longer exist. The only interface state to be left is a down state invading an up state, represented by the lower branch. Since this

interface state is an attractor of the dynamics the circular up state domain will cease expanding and begin shrinking. This is an example of a spontaneous transition between the counterpropagating interface states, induced by curvature.

Spontaneous interface transitions provide the mechanism of a new growth mode in which a non-circular growing domain splits into two parts which grow and split again in a process reminiscent of cell division. A numerical demonstration of this growth mode is shown in Fig. 8. The initial up state domain in this simulation is not perfectly circular, but has some oval shape. As the domain grows the flatter parts of its boundary reach the end point of the upper branch in Fig. 7 sooner and are the first to undergo interface transitions. Along with these transitions spiral-wave pairs nucleate, a pair at the two edges of any interface segment that underwent a transition (see discussion above). The spontaneous nucleation of spiral waves deforms

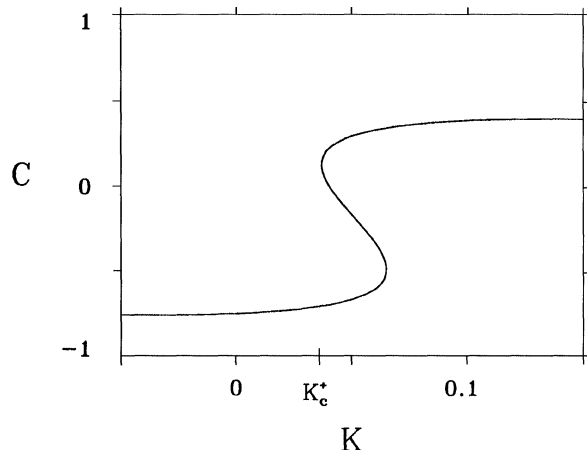


FIGURE 7 A multivalued relation between the front velocity and its curvature for the parameters used in the domain splitting simulation shown in Fig. 8.

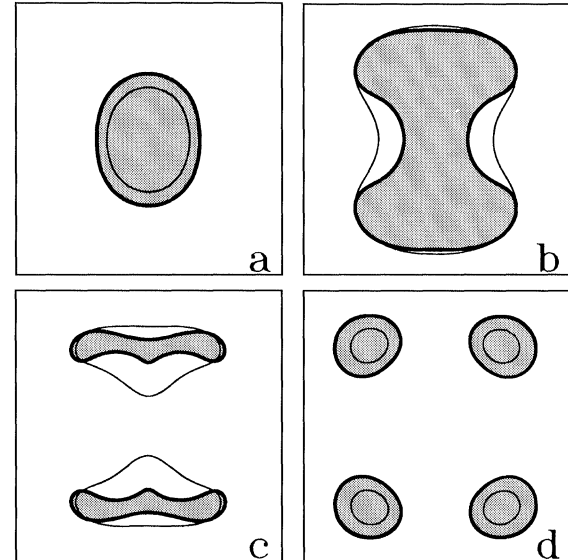


FIGURE 8 Domain splitting induced by curvature variations in time. Local front transitions occur at the flatter portions of the expanding front. They are accompanied by the nucleation of pairs of spiral waves (the crossing points of the thick and thin lines), and followed by domain splitting. The pictures were obtained by numerical integration of Eq. (5) close to the front bifurcation. Parameters: $a_0 = -0.15$, $a_1 = 2.0$, $\epsilon = 0.014$, $\delta = 3.5$.

the up state domain and leads to its splitting. Similar domain splitting phenomena have recently been observed in chemical reactions [15]. More details about this phenomenon can be found in [16,17]. A necessary condition for this growth mode is marginal stability, or instability to transverse perturbations (see below) to prevent a rapid convergence of the domain to a circular form.

3.2 A Transverse Instability

Interfaces in two-dimensional systems may become unstable also to transverse perturbations, that is, perturbations leading to a curved interface. Imagine a straight interface perturbed locally so as to have a bulge. In the course of time this bulge may smooth out and disappear if the interface is stable, or grow into a finger if it is sufficiently unstable. This instability is analyzed in the Appendix and demonstrated numerically in Fig. 9. Shown in this figure is a simulation of Eq. (5), starting from an almost flat interface. The interface initially develops bulges which then grow into fingers and tip split. The split

tips grow into pairs of fingers and the process continues until a stationary labyrinth fills the whole system. The simulation was carried out far from the front bifurcation, in the single front regime ($\eta > \eta_c$). Approaching the bifurcation would result in domain splitting and possibly domain merging as well.

The final labyrinthine pattern is an attractor of the dynamics, one out of many other attractors, all having the same qualitative appearance but differing in quantitative details. The labyrinthine pattern shown in Fig. 1 suggests the existence of a transverse instability of the interface separating high and low acidity domains. Transverse instabilities often develop when the interface motion triggers a process that acts to slow down the speed of propagation. If this process is diffusing fast enough to the two sides of an initial bulge it may slow down the propagation of those parts of the interface and let the bulge grow.

A similar scenario holds for almost circular domains and provides another possible growth mode. We can distinguish now among three different growth modes. (i) *Even growth*, where the boundary of the growing domain retains a circular shape. This mode is realized away from the front bifurcation (on either side) and below the transverse instability. (ii) *Domain splitting*, where the growth is accompanied by splitting into disjoint domains. The conditions for this growth mode are proximity to the front bifurcation and marginal stability or instability to transverse perturbations. (iii) *Fingering and tip splitting*, where the domain grows fingers which split into pairs of fingers and so on. Fingering occurs far above the transverse instability and far away from the front bifurcation, in the single front regime.

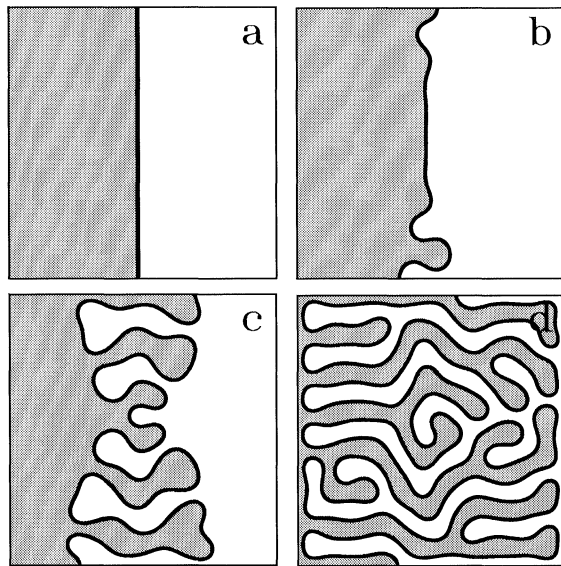


FIGURE 9 Numerical simulations of Eq. (5) deep in the single front regime and beyond the transverse instability of that front. Like in the chemical experiment (Fig. 1), the transverse instability leads eventually to a stationary labyrinth.

4 DISCUSSION

The question of predicting and controlling the urban environment has repeatedly been addressed by modern geographers (see the recent review by Portugali [19]). During the post World War II years a positivistic approach prevailed. It was widely believed that the exact and the engineering sciences

can advance our understanding of the built environment and provide *quantitative* means to plan and control it. This approach did not last for too long. The disillusionment came by the end of the 60s and early 70s when it was realized that the urban environment is far more complex to be handled globally and quantitatively with scientific methods. Geographers turned toward social theories attempting to apply abstract concepts to practical environmental issues. Gradually it became evident that this approach too is remote from reality, and a renewed interest in positivism has begun [19]. Concepts taken from the realm of exact sciences, like chaos, fractals, self-organization, synergetics and so on, have started pervading into the language and conceptual approach of geographers. In light of the huge impact these concepts have had on a variety of scientific disciplines dealing with complex natural phenomena, it was not surprising to find these concepts diffusing to studies of complex systems outside the strict realm of exact sciences.

The global, quantitative scientific approach has rightfully been abandoned, but a *qualitative* approach [1] based on the concepts and tools of nonlinear dynamics may still prove successful. In addressing the question of sociocultural segregation, for example, we need not take into account all aspects of the urban environment. It might be sufficient to include only those considerations needed to capture the essential bifurcations and instabilities, in this case, the front bifurcation and the transverse instability. A qualitative approach also resolves the problem of quantifying human variables such as tolerance to individuals belonging to different sociocultural groups. Since the ultimate interest is in qualitative features, assigning numbers to human variables is merely a mean to take full advantage of the advanced mathematical theory of nonlinear dissipative systems.

Can we predict or control urban behaviors? Evidently not in any quantitative sense. But we might be able to identify factors that affect the qualitative behavior of the system and in this sense predict or control urban behaviors. Mathematical modeling, that focuses on restricted aspects of

the urban environment and captures the essential instabilities and bifurcations, may help achieving this goal. Returning to the issue of sociocultural segregation, a CA model in the spirit of the City can be used to predict which of the three growth modes, *even*, *domain splitting* or *fingering*, is likely to occur in the modeled environment. The model, which should capture the two interface instabilities, can also suggest ways to control the growth rate by identifying the urban factors that move the system toward or across these instabilities.

Acknowledgments

I am thankful to Aric Hagberg for his assistance in producing some of the figures of this paper. The mathematical part of this paper, in particular the Appendix, is based on previous works with Aric Hagberg. This work was supported in part by the Israel Ministry of Science and the Arts research.

References

- [1] P.M. Allen, M. Sanglier, G. Engelen and F. Boon, *Environment and Planning B* **12**, 65 (1985).
- [2] W. Weidlich, "Synergetics and Social Science", in *Lasers and Synergetics*, R. Graham and A. Wunderline, eds. (Springer, Berlin, 1987).
- [3] K.J. Lee, W.D. McCormick, Q. Ouyang and H.L. Swinney, *Science* **261**, 192 (1993).
- [4] K.J. Lee and H.L. Swinney, *Phys. Rev. E* **51**, 1899 (1995).
- [5] J. Portugali, I. Benenson and I. Omer, *Geographical Analysis* **26**, 321 (1994).
- [6] S. Wolfram, *Physica D* **10**, 1 (1984).
- [7] P. Manneville, N. Boccara, G.Y. Vichniac and R. Bidaux, eds. *Cellular Automata and Modeling Physical Systems* (Springer, Berlin, 1989).
- [8] M. Gerhardt, H. Schuster and J.J. Tyson, *Science* **247**, 1563 (1990).
- [9] W.-B. Zhang, *Geographical Analysis* **21**, 91 (1989).
- [10] J. Guckenheimer and P. Holmes, *Nonlinear Oscillations, Dynamical Systems and Bifurcations in Vector Fields* (Springer, New York, 1983).
- [11] Y. Nishiura and M. Mimura, *SIAM J. Appl. Math.* **49**, 481 (1989).
- [12] P. Coullet, J. Lega, B. Houchmanzadeh and J. Lajzerowicz, *Phys. Rev. Lett.* **65**, 1352 (1990).
- [13] A. Hagberg and E. Meron, *Phys. Rev. E* **48**, 705 (1993).
- [14] A. Hagberg and E. Meron, *Nonlinearity* **7**, 805 (1994).
- [15] M. Bode, A. Reuter, R. Schmeling and H.-G. Purwins, *Phys. Lett. A* **185**, 70 (1994).
- [16] K.J. Lee, W.D. McCormick, H.L. Swinney and J.E. Pearson, *Nature* **369**, 215 (1994).
- [17] A. Hagberg and E. Meron, *Chaos* **4**, 477 (1994).
- [18] C. Elphick, A. Hagberg and E. Meron, *Phys. Rev. E* **51**, 3052 (1995).

- [19] A. Hagberg and E. Meron, *Phys. Rev. Lett.* **72**, 2494 (1994).
- [20] J. Portugali, *The Taming of the Shrew Environment*, preprint (1995).
- [21] E. Meron, *Physics Reports* **218**, 1 (1992).
- [22] J.J. Tyson and J.P. Keener, *Physica D* **32**, 327 (1988).
- [23] G. Haas, M. Bär, I.G. Kevrekidis, P.B. Rasmussen, H.-H. Rotermund and G. Ertl, *Phys. Rev. Lett.* **75**, 3560 (1995).
- [24] Y.A. Rzhanov, H. Richardson, A.A. Hagberg and J.V. Moloney, *Phys. Rev. A* **47**, 1480 (1993).
- [25] M. Bode, A. Reuter, R. Schmeling and H.-G. Purwins, *Phys. Lett. A* **185**, 70 (1994).
- [26] B.S. Kerner and V.V. Osipov, *Sov. Phys. Usp.* **32**, 101 (1989).
- [27] D.A. Kessler and H. Levine, *Phys. Rev. A* **41**, 5418 (1990).
- [28] T. Ohta, M. Mimura and R. Kobayashi, *Physica D* **34**, 115 (1989).
- [29] D. Horváth, V. Petrov, S.K. Scott and K. Schowalter, *J. Chem. Phys.* **98**, 6332 (1993).

APPENDIX

To study the front bifurcation and the transverse instability for continuous systems we consider a reaction–diffusion model for two scalar variables u and v :

$$\begin{aligned} u_t &= u - u^3 - v + \nabla^2 u, \\ v_t &= \epsilon(u - a_1 v - a_0) + \delta \nabla^2 v, \end{aligned} \quad (5)$$

where the subscript t denotes the partial derivative with respect to t and ∇^2 is the two dimensional Laplacian operator. This type of model has been studied in the context of nerve conduction (with $\delta = 0$) and chemical reactions [20–22], semiconductor resonators [23], chains of coupled oscillators [24] and many other systems [25]. It is an extension of (3) in the sense that the constant parameter b is now a second dynamical variable (v). Equations (5) contains four parameters: ϵ , the ratio of the time scales associated with the two variables, δ , the ratio of the diffusion constants, and two parameters, $a_1 > 0$ and a_0 , that determine the number and type of homogeneous steady states. These states are found by the intersections of the nullclines $v = u - u^3$ and $v = (u - a_0)/a_1$. For this study we always choose a_1 and a_0 so that there are three intersections, each on a different branch of the cubic nullcline. The intersections on the outer branches represent stable solutions which we will call (u_+, v_+) for the positive branch “up” state, and

(u_-, v_-) for the negative branch “down” state. When $a_0 = 0$, Eq. (5) has an odd symmetry and $(u_+, v_+) = -(u_-, v_-)$.

We focus here on the regime $\epsilon/\delta \ll 1$ where a singular perturbation analysis of (5) can be performed. For large ϵ/δ a different approach can be used [14]. In addition to the two stable homogeneous solutions, Eq. (5) also admits front solutions connecting regions of (u_+, v_+) and (u_-, v_-) . The stability and type of these fronts depend upon the size of both ϵ and δ . Decreasing from large ϵ , a bifurcation from a single front solution to three front solutions occurs. For δ sufficiently small, the single front solution below the front bifurcation and two of the three solutions beyond the bifurcation are stable. Any of these front solutions undergoes a transverse instability as δ is increased past a critical value.

The Front Bifurcation

To study the front bifurcation we consider one-dimensional (along the x axis) front solutions propagating at constant speeds and connecting the up state at $-\infty$ to the down state at $+\infty$. The solutions satisfy

$$\begin{aligned} \mu u_{\zeta\zeta} + c\delta\mu u_{\zeta} + u - u^3 - v &= 0, \\ v_{\zeta\zeta} + cv_{\zeta} + u - a_1 v - a_0 &= 0, \end{aligned} \quad (6)$$

where we rescaled space and time according to

$$z = \sqrt{\mu}x, \quad \tau = \epsilon t, \quad \mu = \epsilon/\delta \ll 1, \quad (7)$$

and introduced the traveling frame coordinate $\zeta = z - c\tau$. Front solutions of (6) can be separated into two parts pertaining to distinct regions: outer regions, away from the front, where both u and v vary on a scale of $\mathcal{O}(1)$, and an inner region, including the front, where u varies much faster than v . In the outer regions the derivative terms in the first equation of (6) can be neglected leading to the solutions $u = u_{\pm}(v)$ of the remaining cubic relation $u - u^3 - v = 0$. Using these forms in the second equation of (6), and setting the front position, $u = 0$,

at the origin, $\zeta = 0$, we obtain closed equations for v ,

$$v_{\zeta\zeta} + cv_{\zeta} + u_{\pm}(v) - a_1 v - a_0 = 0, \quad (8)$$

with $u = u_+(v)$ when $\zeta < 0$ and $u = u_-(v)$ when $\zeta > 0$. To simplify, we choose a_1 large enough so that $v \ll 1$ and the branches $u_{\pm}(v)$ can be approximated by the linear forms $u_{\pm}(v) = \pm 1 - v/2$. We then obtain the following linear boundary value problems for the two outer regions:

$$\begin{aligned} \zeta < 0: \quad & v_{\zeta\zeta} + cv_{\zeta} - q^2 v + q^2 v_+ = 0, \\ & v(0) = v_f, \quad v(-\infty) = v_+, \\ \zeta > 0: \quad & v_{\zeta\zeta} + cv_{\zeta} - q^2 v + q^2 v_- = 0, \\ & v(0) = v_f, \quad v(\infty) = v_-, \end{aligned} \quad (9)$$

where

$$v_{\pm} = \frac{\pm 1 - a_0}{a_1 + \frac{1}{2}}, \quad q^2 = a_1 + \frac{1}{2}, \quad (10)$$

and v_f is the level of v at the front position. The solutions are

$$\begin{aligned} v(\zeta) &= (v_f - v_+) e^{\sigma_1 \zeta} + v_+, \quad \zeta < 0, \\ v(\zeta) &= (v_f - v_-) e^{\sigma_2 \zeta} + v_-, \quad \zeta > 0, \end{aligned} \quad (11)$$

with

$$\sigma_{1,2} = -c/2 \pm (c^2/4 + q^2)^{1/2}. \quad (12)$$

By construction, the two outer solutions for v are continuous at $\zeta = 0$. Matching the derivatives of v at $\zeta = 0$ gives a relation between c , the speed of the front, and v_f , the value of the v field at the front position,

$$v_f = -\frac{c}{2q^2(c^2/4 + q^2)^{1/2}} - \frac{a_0}{q^2}. \quad (13)$$

A second relation between v_f and c is obtained by solving the inner problem. In the front region u varies on a scale of $\mathcal{O}(\sqrt{\mu})$ but variations of v are still on a scale of $\mathcal{O}(1)$. Stretching the traveling-frame coordinate according to $\chi = \zeta/\sqrt{\mu}$ we obtain from (5)

$$\begin{aligned} u_{\chi\chi} + \eta c u_{\chi} + u - u^3 - v &= 0, \\ v_{\chi\chi} + \sqrt{\mu} c v_{\chi} + \mu(u - a_1 v - a_0) &= 0, \end{aligned} \quad (14)$$

where $\eta^2 = \epsilon\delta$. Setting $\mu = 0$ in the second equation of (14) gives the equation $v_{\chi\chi} = 0$, and we choose the solution $v = \text{constant}$. Fixing the constant, $v = v_f$, in the equation for u gives a nonlinear eigenvalue problem for c ,

$$u_{\chi\chi} + \eta c u_{\chi} + f(u, v_f) = 0, \quad u(\mp\infty) = u_{\pm}(v_f), \quad (15)$$

with $f(u, v_f) = u - u^3 - v_f$. The cubic function, f , can be rewritten as

$$f(u, v_f) = -[u - u_-(v_f)][u - u_0(v_f)][u - u_+(v_f)], \quad (16)$$

where $u_-(v_f) = -1 - v_f/2$, $u_0 = v_f$, and $u_+(v_f) = 1 - v_f/2$, are the linearized forms of the cubic isocline near the three solutions $u = -1, 0, 1$ respectively. The speed of the front solution of (15) is

$$\eta c = \left(\frac{1}{\sqrt{2}}\right)(u_+ - 2u_0 + u_-) = \left(\frac{-3}{\sqrt{2}}\right)v_f. \quad (17)$$

Combining the two equations, (13) and (17), we find an implicit relation for the front speed, c , in terms of the equation parameters η, a_1 , and a_0 ,

$$\frac{\sqrt{2}}{3} \eta c = \frac{c}{2q^2\sqrt{c^2/4 + q^2}} + \frac{a_0}{q^2}. \quad (18)$$

This equation was derived using the coordinate scaling (7). The relation for the original variables x and t is found by replacing $c \rightarrow c/\eta$ in (18):

$$c = \frac{3c}{\sqrt{2}q^2\sqrt{c^2 + 4\eta^2q^2}} + c_{\infty}, \quad (19)$$

where $c_{\infty} = 3a_0/\sqrt{2}q^2$.

For the symmetric case, $a_0 = 0$ and consequently $c_{\infty} = 0$. Equation (19) then has the solution $c = 0$ representing a stationary front. This solution exists for all η values. When $\eta < \eta_c = \frac{3}{2}\sqrt{2}q^3$ two additional solutions $c = \pm 2q\sqrt{\eta_c^2 - \eta^2}$ appear, representing counterpropagating fronts. Figure 5 (left) displays the corresponding pitchfork bifurcation.

For the nonsymmetric case we solved (19) numerically. A plot of the solutions, $c=c(\eta)$, in the (c, η) plane yields the imperfect pitchfork bifurcation diagram shown in Fig. 5 (right). The bifurcation point, $\eta=\eta_c$, occurs for smaller critical η value than the symmetric case and the front that exists for $\eta > \eta_c$ is not stationary.

The Effect of Curvature and the Transverse Instability

For δ sufficiently large, planar front solutions may become unstable to transverse or curvature perturbations [26–28]. To study the transverse instabilities of the various front solutions we change from the fixed coordinate system to a coordinate system moving with the front. Let $X=(X, Y)$ be the position vector of the front represented by the $u=0$ contour line. The moving coordinate frame (r, s) is defined by the relation

$$\mathbf{x} = (x, y) = X(s, t) + r\hat{\mathbf{r}}(s, t), \quad (20)$$

with the coordinate s parameterizing the direction along the front and $\hat{\mathbf{r}} = (Y_s \hat{\mathbf{x}} - X_s \hat{\mathbf{y}}) / \sqrt{X_s^2 + Y_s^2}$, the unit vector normal to the front (the subscript s denotes partial derivatives with respect to s). We assume the front radius of curvature is much larger than $l_v = \sqrt{\delta/\epsilon}$, the scale of v variations across the front. We also assume the curvature varies slowly both along the front direction and in time. With these assumptions Eq. (5) assumes the form

$$\begin{aligned} u_{rr} + (c_r + \kappa)u_r + u - u^3 - v &= 0, \\ \delta v_{rr} + (c_r + \delta\kappa)v_r + \epsilon(u - a_1 v - a_0) &= 0, \end{aligned} \quad (21)$$

where $\kappa(s, t) = X_s Y_{ss} - Y_s X_{ss}$ is the front curvature, and $c_r(s, t) = X_t \cdot \hat{\mathbf{r}}$ is the front normal velocity.

Multiplying the second equation of (21) by the factor $\Delta(s, t) = (c_r + \kappa)/(c_r + \delta\kappa)$ gives

$$\begin{aligned} u_{rr} + (c_r + \kappa)u_r + u - u^3 - v &= 0, \\ \tilde{\delta}v_{rr} + (c_r + \kappa)v_r + \tilde{\epsilon}(u - a_1 v - a_0) &= 0, \end{aligned} \quad (22)$$

with $\tilde{\epsilon} = \epsilon\Delta$ and $\tilde{\delta} = \delta\Delta$. This system is exactly of the same form as Eq. (5) for a planar ($\kappa=0$) front propagating at constant speed, $c_r + \kappa$, in the normal direction, $\hat{\mathbf{r}}$, except the original parameters ϵ and δ are replaced by effective parameters $\tilde{\epsilon}$ and $\tilde{\delta}$. The front bifurcation formula (19) can now be applied to show the effects of curvature on the front velocity. Using this formula with c replaced by $c_r + \kappa$ and η by $\tilde{\eta} = \eta\Delta$ we obtain an implicit relation for the normal front velocity in terms of its curvature,

$$c_r + \kappa = \frac{3(c_r + \delta\kappa)}{\sqrt{2}q^2[(c_r + \delta\kappa)^2 + 4\eta^2q^2]^{1/2}} + c_\infty. \quad (23)$$

A plot of c_r versus κ in the vicinity of the front bifurcation yields a multivalued relation as depicted in Fig. 8.

Equation (23) can be used to study the stability of the planar fronts to transverse perturbations. We look for a linear velocity curvature relation,

$$c_r = c_0 - d\kappa + \mathcal{O}(\kappa^2), \quad (24)$$

valid for small curvature. Here $c_0(\eta)$ is the speed of a planar front satisfying (19). A positive (negative) sign of the coefficient d implies stability (instability) to transverse perturbations. Inserting (24) into the expression for the front speed, keeping only linear terms, we find,

$$\begin{aligned} d &= \frac{1}{\alpha} + \left(1 - \frac{1}{\alpha}\right)\delta, \\ \alpha &= 1 - \frac{c_0 - c_\infty}{c_0} \left(1 - \frac{2q^4}{9}(c_0 - c_\infty)^2\right). \end{aligned} \quad (25)$$

For each planar solution branch, $c_0 = c_0(\eta)$, the condition $d=0$ defines a line in the $\epsilon - \delta$ plane where the corresponding planar front branch undergoes a transverse instability. Setting $d=0$ for the symmetric case ($a_0=0$), the stationary and counter-propagating fronts become unstable to transverse modulations when $\delta > \frac{8}{9}q^6\epsilon$ and $\delta > 3/(2\sqrt{2}q^3\sqrt{\epsilon})$, respectively.

Special Issue on Intelligent Computational Methods for Financial Engineering

Call for Papers

As a multidisciplinary field, financial engineering is becoming increasingly important in today's economic and financial world, especially in areas such as portfolio management, asset valuation and prediction, fraud detection, and credit risk management. For example, in a credit risk context, the recently approved Basel II guidelines advise financial institutions to build comprehensible credit risk models in order to optimize their capital allocation policy. Computational methods are being intensively studied and applied to improve the quality of the financial decisions that need to be made. Until now, computational methods and models are central to the analysis of economic and financial decisions.

However, more and more researchers have found that the financial environment is not ruled by mathematical distributions or statistical models. In such situations, some attempts have also been made to develop financial engineering models using intelligent computing approaches. For example, an artificial neural network (ANN) is a nonparametric estimation technique which does not make any distributional assumptions regarding the underlying asset. Instead, ANN approach develops a model using sets of unknown parameters and lets the optimization routine seek the best fitting parameters to obtain the desired results. The main aim of this special issue is not to merely illustrate the superior performance of a new intelligent computational method, but also to demonstrate how it can be used effectively in a financial engineering environment to improve and facilitate financial decision making. In this sense, the submissions should especially address how the results of estimated computational models (e.g., ANN, support vector machines, evolutionary algorithm, and fuzzy models) can be used to develop intelligent, easy-to-use, and/or comprehensible computational systems (e.g., decision support systems, agent-based system, and web-based systems)

This special issue will include (but not be limited to) the following topics:

- **Computational methods:** artificial intelligence, neural networks, evolutionary algorithms, fuzzy inference, hybrid learning, ensemble learning, cooperative learning, multiagent learning

- **Application fields:** asset valuation and prediction, asset allocation and portfolio selection, bankruptcy prediction, fraud detection, credit risk management
- **Implementation aspects:** decision support systems, expert systems, information systems, intelligent agents, web service, monitoring, deployment, implementation

Authors should follow the Journal of Applied Mathematics and Decision Sciences manuscript format described at the journal site <http://www.hindawi.com/journals/jamds/>. Prospective authors should submit an electronic copy of their complete manuscript through the journal Manuscript Tracking System at <http://mts.hindawi.com/>, according to the following timetable:

Manuscript Due	December 1, 2008
First Round of Reviews	March 1, 2009
Publication Date	June 1, 2009

Guest Editors

Lean Yu, Academy of Mathematics and Systems Science, Chinese Academy of Sciences, Beijing 100190, China; Department of Management Sciences, City University of Hong Kong, Tat Chee Avenue, Kowloon, Hong Kong; yulean@amss.ac.cn

Shouyang Wang, Academy of Mathematics and Systems Science, Chinese Academy of Sciences, Beijing 100190, China; sywang@amss.ac.cn

K. K. Lai, Department of Management Sciences, City University of Hong Kong, Tat Chee Avenue, Kowloon, Hong Kong; mskklai@cityu.edu.hk